Health Monitoring for Damage Initiation & Progression during Mechanical Shock in Electronic Assemblies

Pradeep Lall, Prakriti Choudhary, Sameep Gupte, Jeff Suhling
Auburn University
Department of Mechanical Engineering
And Center for Advanced Vehicle Electronics
Auburn, AL 36849
Tele: (334) 844-3424
E-mail: lall@eng.auburn.edu

Abstract
Electronic products may be subjected shock and vibration during shipping, normal usage and accidental drop. High-strain rate transient bending produced by such loads may result in failure of fine-pitch electronics. Current experimental techniques rely on electrical resistance for determination of failure. Significant advantage can be gained by prior knowledge of impending failure for applications where the consequences of system-failure may be catastrophic. This research effort focuses on an alternate approach to damage-quantification in electronic assemblies subjected to shock and vibration, without testing for electrical continuity. The proposed approach can be extended to monitor product-level damage.

In this paper, statistical pattern recognition and leading indicators of shock-damage have been used to study the damage initiation and progression in shock and drop of electronic assemblies. Statistical pattern recognition is currently being employed in a variety of engineering and scientific disciplines such as biology, psychology, medicine, marketing, artificial intelligence, computer vision and remote sensing [Jain, et. al. 2000]. The application quantification of shock damage in electronic assemblies is new.

Previously, free vibration of rectangular plates has been studied by various researchers [Leissa 1969, Young 1950, Gorman 1982, Gurgoze 1984, Wu 2003] for development of analytical closed-form models. In this paper, closed-form models have been developed for the eigen-frequencies and mode-shapes of electronic assemblies with various boundary conditions and component placement configurations. Model predictions have been validated with experimental data from modal analysis. Pristine configurations have been perturbed to quantify the degradation in confidence values with progression of damage. Sensitivity of leading indicators of shock-damage to subtle changes in boundary conditions, effective flexural rigidity, and transient strain response have been quantified. A damage index for Experimental Damage Monitoring has been developed using the failure indicators.

The above damage monitoring approach is not based on electrical continuity and hence can be applied to any electronic assembly structure irrespective of the interconnections. The damage index developed provides parametric damage progression data, thus removing the limitation of current failure testing, where the damage progression can not be monitored. Hence the proposed method does not require the assumption that the failure occurs abruptly after some number of drops and can be extended to product level drops.

Introduction
Damage due to shock and vibration on portable products may manifest in solder interconnects and copper traces. The damage may be due to overstress or cumulative. The objective of this paper is to investigate the use of statistical pattern recognition to study the affect of damage due to drop and impact on the reliability of electronic devices. Statistical pattern recognition is currently being employed in a variety of engineering and scientific disciplines such as biology [Christodoulou, et. al. 1999], psychology [Dellaert, et. al. 1996], medicine [Holt, et. al. 1998], marketing [Apte 1997], artificial intelligence [Kohonen, et. al. 1988], computer vision [Low, et. al. 1990] and remote sensing [Jain, et. al. 2000]. The use of mahalanobis-distance and wavelet-packet energy approaches, coupled with analytical closed-form solutions for health-monitoring has been studied. It is has been shown that variation of effective-geometry and design-parameters, coupled with statistical pattern recognition techniques can enable in-situ quantification and sensing of damage initiation and progression.

Structural health monitoring, i.e. the process of establishing knowledge of the current condition of a structure has found application in various fields, like shaft crack detection [Lebold, et. al. 2004, Gyekenyesi, et. al. 2003] and aircraft maintenance [Hedley, et. al. 2004, Hickman, et. al. 1991, Castanien, et. al. 1996]. This method also finds application in performance assessment of Machinery systems [Lee 1995, Chuang, et. al. 2004, Wegerich 2003]. While, structural health monitoring is popularly used in various fields, its application to the field of reliability of electronic structures is new. The relevant features, like vibration, temperature etc. are extracted from strategically placed sensors on the machine structure, and the algorithms developed for performance assessment of a system are applied. Experience in other applications indicates that structural health monitoring produces gains in the performance and cost-effective maintenance of high-value assets such as aircrafts, civil infrastructure and maritime vessels. Structural health monitoring systems help in reduction of down-time and elimination of component tear-down inspections, thus reducing the risk of failure during operation.

Currently the main reliability tests performed on electronic assemblies undergoing drop and shock are the JEDEC drop

test [Lall, et. al. 2005], Shear testing [Hanabe, et. al. 2004] and ball pull testing [Newman 2005]. The JEDEC drop test is based on the JEDEC test standards, and studies the affect of drop and shock experimentally on Test boards. These tests are limited to board level drops with the packages on the board connected in a daisy chain as the experimental techniques relies on measurement of electrical resistance for determination of failure. Ball-pull testing and Shear testing has also been applied to test structures to study the reliability of electronic assemblies to drop and shock environment. These tests study the impact toughness of solder joints quantitatively by means of various tests including Charpy test [Date, et. al. 2004], Shear test, and the package to board interconnection shear strength (PBISS) technique [Hanabe, et. al. 2004]. The above mentioned test procedures cannot monitor the damage occurring during shock and drop, hence they cannot be used for health monitoring of electronic assemblies.

In this paper the electronic assembly is modeled as a rectangular board with point masses on it, representing the PCB with the packages attached to it. Various kinds of boundary conditions have been studied, determined by the packaging of the assembly at the product level. Hence a press fit edge of a PCB is modeled as a clamped edge condition, while a configuration with screws attaching the PCB to the casing is modeled as a plate having point supports. In this paper, the JEDEC drop test assembly has been modeled as a rectangular plate on rigid point supports, with packages being modeled as attached masses on the PCB. The vibrational frequency and mode shapes have been correlated with FEM models developed for JEDEC drop testing and also with experimental data obtained during the tests. Various Case studies of failure occurring due to change in effective attributes of the assembly have been discussed and damage monitoring done to show damage progression.

The closed form approach has been used in conjunction with the FE approach, so as to under sensitivity of various effective parameters that affect the dynamic parameters of the electronic assemblies. Damage in interconnects has been correlated with static, quasi-static and dynamic response of the assemblies.

Table 1: Test Vehicles

	Tape Array BGA	Plastic BGA	Chip Array BGA	Flex BGA	Plastic BGA	Tape Array BGA
Pkg Size (mm)	10	27	7	16	15	6
I/O	144	676	84	280	196	64
Pitch (mm)	0.8	1	0.5	0.8	1	0.5
Die Size (mm)	7	6.35	5.4	10	6.35	4
Substrate Thick (mm)	0.36	0.36	0.36	0.36	0.36	0.36
Substrate Pad Dia.	0.3	0.38	0.28	0.3	0.38	0.28
Substrate Pad	NSMD	SMD	NSMD	NSMD	SMD	NSMD
Ball Diameter (mm)	0.48	0.63	0.48	0.48	0.5	0.32

Test Vehicle

The test board has been used to study the reliability of fine-pitch ball-grid arrays in transient-shock. The packages on the test board are 27 mm ball-grid array, 1 mm pitch, 676 I/O; 10 mm Tape Array, 0.8 mm pitch, 144 I/O; 16 mm Flex BGA, 0.8 mm pitch, 280 I/O; 7 mm CABGA, 0.5 mm pitch, 84 I/O; 15 mm ball-grid array, 1 mm pitch, 196 I/O; 6mm Tape Array, 0.5 mm pitch, 64 I/O. (Table 1). Each component has multiple components. All the components are mounted on one side of the board. The test board is made of FR-4. The test board is based on standard PCB technology with no build-up or HDI layers. Test Board is 5.5" by 8" by 0.0591" thick.

Development of Training Signal and High-Speed Measurement Transient Dynamic Response

The test boards were subjected to a controlled drop. Repeatability of drop orientation is critical to measuring a repeatable response and develop a training signal for statistical pattern recognition. Small variations in the drop orientation can produce vastly varying transient-dynamic board responses. Significant effort was invested in developing a repeatable drop set-up. The drop height was varied from 3 feet to 6 feet. Component locations on the test boards were instrumented with strain sensors. Strain and continuity data was acquired during the drop event using a high-speed data acquisition system at 2.5 to 5 million samples per second. The drop-event was simultaneously monitored with ultra high-speed video camera operating at 50,000 frames per second. Targets were mounted on the edge of the board to allow high-speed measurement of relative displacement during drop.

The test boards were dropped in their vertical orientation with a weight attached to its top edge (Figure 1). The board orientation during drop has been maintained to be close to zero degrees with the vertical. In addition, the boards were dropped in the horizontal orientation per the JESD22-B111. Strain, displacement, orientation angle, velocity, acceleration, and continuity data has been acquired simultaneously.

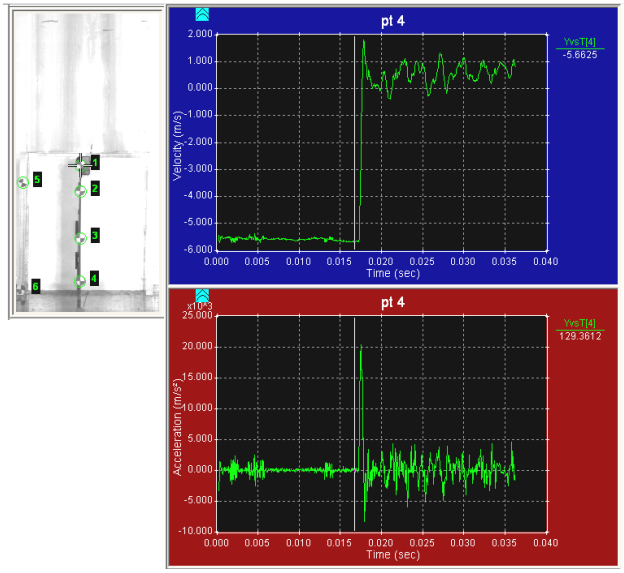

Figure 1: Measurement of Velocity, Acceleration, and Relative Displacement During Impact.

An image tracking software was used to quantitatively measure displacements during the drop event. Figure 1 shows a typical angle, and relative displacement plot measured during the drop event. The position of the vertical line in the plot represents the present location of the board (i.e. just prior to impact in this case) in the plot with "pos (m)" as the ordinate axis. The plot trace subsequent to the white scan is the relative displacement of the board targets w.r.t. to the specified reference. Figure 2 shows the board instrumentation for strain and relative displacement during horizontal JEDEC drop. In addition to relative displacement, velocity, and acceleration of the board prior to impact was measured. This additional step was necessary since, the boards were subjected to a controlled drop, in order to reduce variability in drop orientation. The measured velocity prior to impact was used to correlate the controlled drop height to free-drop height ($v = \sqrt{2gh}$). Thus velocity prior to impact for a 6ft drop (≈ 1.83 meter) will be 5.99 m/s.

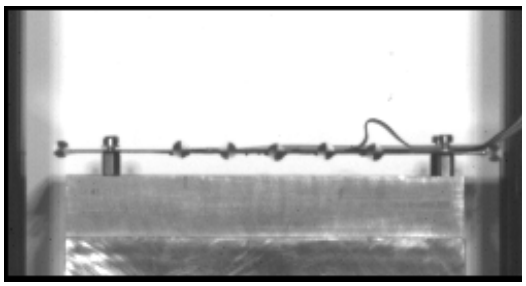

Figure 2: Relative Displacement and Strain Measurement in Horizontal Orientation.

Statistical Pattern Recognition

Statistical Pattern Recognition refers to the study of algorithms that recognize patterns in data and contains various sub disciplines like discriminant analysis, feature extraction, error estimation, and cluster analysis. Some important application areas of statistical pattern recognition are image analysis, character recognition, speech analysis, man and machine diagnostics, person identification and industrial inspection. Statistical pattern recognition has been developed using several methods and applied to plethora of applications including neural networks applied to faults in gas turbine engines [Atlas 1996, Sick 1998, Chuang 2004], hidden markov models applied to speech recognition and machine tool wear [Wang 2002, Heck 1991], multivariate similarity models applied to machine health monitoring [Wegerich 2003], auto-regression models applied to machine health monitoring [Logan 2003, Shao 2000, Lei 2003, Casoetto 2003, Yan 2005, Engel 2000], wavelet packet approach applied to tool wear [Yan 2004], FFT based frequency-domain analysis applied to machine monitoring [Yuan 2004], time-series methods applied to machine tool monitoring [Zheng 1992, Djurdjanovic 2002], and statistical data comparison applied to railway bearing diagnostics [National Research Council Canada 1999]. Application of statistical pattern recognition to health monitoring of electronic assemblies subjected to shock and vibration environments is new.

In this paper statistical pattern recognition is used to study the degradation of reliability in electronic assemblies, due to shock and drop. The health monitoring of assemblies has been accomplished by monitoring the confidence values computed by applying statistical pattern recognition techniques to the transient-strain response, transient displacement-response, vibration mode shapes and frequencies of the electronic assembly under shock and drop. Correlation of structural response, damage proxies and underlying damage has been accomplished with closed-form models, explicit finite-element models and validated with high-speed experimental data. Here two statistical pattern recognition techniques, including the wavelet packet approach and the Mahalanobis distance approach have been investigated.

Wavelet Packet Approach

Wavelets have been used in several areas including data and image processing [Martin 2001], geophysics [Kumar 1994], power signal studies [Santoso 1996], meteorological studies [Lau 1995], speech recognition [Favero 1994], medicine [Akay 1997], and motor vibration [Fu 2003, Yen 1999]. The wavelet transform is defined by

$$Wf(u,s) = \left\langle f, \psi_{u,s} \right\rangle = \frac{1}{\sqrt{s}} \int_{-\infty}^{+\infty} f(t)\ \psi^*\left(\frac{t-u}{s}\right) dt \qquad (1)$$

where the base atom ψ* is the complex conjugate of the wavelet function which is a zero average function, centered around zero with a finite energy. The function f(t) is decomposed into a set of basis functions called the wavelets with the variables s and u, representing the scale and translation factors respectively.

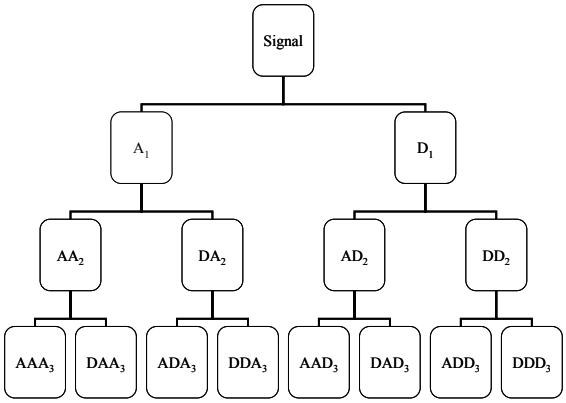

Figure 3 Wavelet Packet Decomposition Framework

The transform has been used to analyze transient strains signals at different frequency bands with different resolutions by decomposing the transient signal into a coarse approximation and detail information (Figure 4). The signal is decimated into different frequency bands by successively filtering the time domain signal using lowpass and highpass filters. The original stress signal is first passed through a halfband highpass filter g[n] and a lowpass filter h[n]. After the filtering, half of the samples are eliminated according to the Nyquist's rule, since the signal now has a highest frequency of p/2 radians instead of p. The signal is therefore subsampled by 2, simply by discarding every other sample. This constitutes one level of decomposition and can mathematically be expressed as follows:

$$y_{high}[k] = \sum_n signal[n] \cdot g[2k-n]$$
$$y_{low}[k] = \sum_n signal[n] \cdot h[2k-n] \quad (2a)$$

where $y_{high}[k]$ and $y_{low}[k]$ are the outputs of the highpass and lowpass filters, respectively, after subsampling by 2. The compression and de-noising in the wavelet packet transform is same as those for a wavelet transform framework. The only difference is that wavelet packets offer a more complex and flexible analysis, because in wavelet packet analysis, the details as well as the approximations are split.

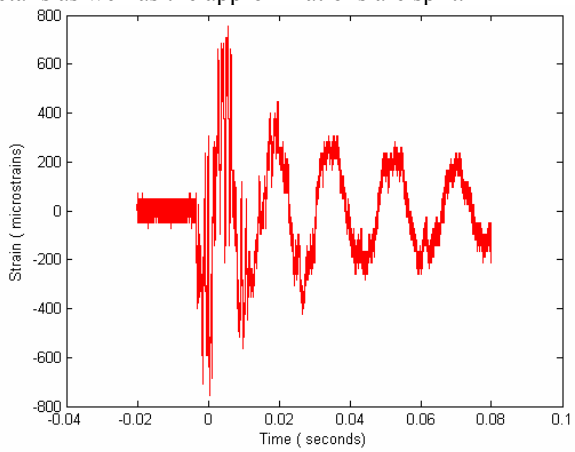

Figure 4: Transient Strain-History at Location of CSP during Drop-Event.

Wavelets have been shown to be useful for texture classification because of their finite length [Lee, et. al. 1995]. If an orthonormal basis is chosen, the wavelet coefficients are independent and possess the distinct features of the original signal. Wavelet packets can be described by the following collection of basis functions, ,

$$W_{2n}(2^{p-1}x - l) = \sqrt{2^{1-p}} \sum_m h(m-2l)\sqrt{2^p}\, W_n(2^p x - m)$$
$$W_{2n+1}(2^{p-1}x - l) = \sqrt{2^{1-p}} \sum_m g(m-2l)\sqrt{2^p}\, W_n(2^p x - m) \quad (2b)$$

where *p* is a scale index, *l* is a translation index, "h" is a low-pass filter, and "g" is a high-pass filter with $g(k) = (-1)^k h(1-k)$. The function $W_0(x)$ can be identified as the low-pass scaling function φ and $W_1(x)$ as the high-pass mother wavelet ψ. A 2-D wavelet packet basis function is given by the product of two 1-D wavelet packet basis along the horizontal and vertical direction. The corresponding 2-D filter coefficients have four groups,

$$hh(k,l) = h(k)h(l)$$
$$hg(k,l) = h(k)g(l)$$
$$gh(k,l) = g(k)h(l)$$
$$gg(k,l) = g(k)g(l) \quad (2c)$$

Wavelet packet basis functions have the properties of smoothness, number of vanishing moments, symmetry, good time and frequency localization, satisfy the admissibility condition and are absolutely square integrable functions.

The discrete wavelets can be classified as non-orthogonal, biorthogonal or orthogonal wavelets. Non-orthogonal wavelets are linearly dependent and redundant frames. Orthogonal wavelets are linearly independent, complete and orthogonal. In the analysis of reliability of electronic assemblies, one of the most widely used wavelets constructed by Daubechies has been applied. The Daubechies wavelets are orthonormal, compactly supported, have maximum number of vanishing moments, and are reasonably smooth. The low-pass and band (high)–pass filter coefficients of the Daubechies wavelets satisfy the conditions of Orthogonality, Normality and Regularity.

An entropy-based criterion is used to select the most suitable decomposition of a given signal. This implies that at each node of the decomposition tree, the information gained by performing a split is quantified. Simple and efficient algorithms exist for both wavelet packet decomposition and optimal decomposition selection. Adaptive filtering algorithms, allow the Wavelet Packet transform to include the "Best Level" and "Best Tree" features that optimize the decomposition both globally and with respect to each node. For obtaining the optimal tree, a node is split into two nodes, if and only if the sum of entropy of the two nodes is lower than the sum of entropy of the initial node. After the wavelet packet transform, the wavelet packet energy is calculated at each node of the decomposition tree. An energy signature E_n for each sequence of wavelet packet coefficients $C^p_{n,k}$, for $n = 0,1,2.....4^{p-1}$ can be computed by using the formula

$$E_n = \frac{1}{N^2} \sum_{k=1}^{N} \left| C_n^p \right|^2 \quad (3)$$

where N is the total number of points in the signal at a given node in the wavelet packet tree, p is the decomposition depth, and C_i is the wavelet packet coefficients obtained during the wavelet packet transform at the particular node where energy is being calculated. The feature vector of length 4^{p-1}, is formed for the signal. The packet energies obtained from the wavelet packet decomposition of the various mode shapes and frequencies of vibration of the electronic assembly are the basis for the computation of confidence values for health monitoring. The Strain signal obtained from sensors placed on the electronic assembly is used to obtain the wavelet packet energy signature. The wavelet packet energy signature for a transient strain signal is shown in Figure 5.

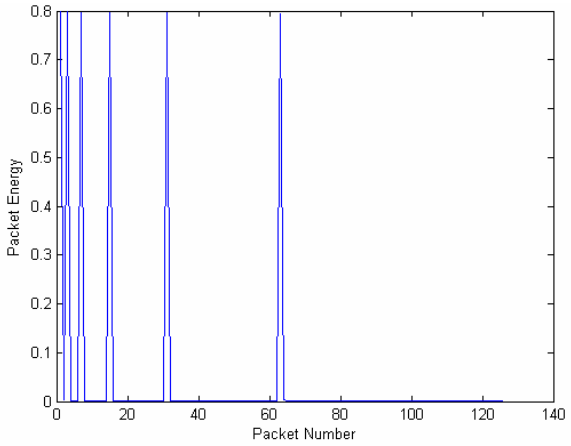

Figure 5: Wavelet packet Energy Signature for the Transient Strain Signal.

Mahalanobis Distance Approach

The Mahalanobis Distance classification is similar to the Maximum Likelihood classification except for the class covariances which are all assumed to be equal, hence the method is more efficient. It is based on correlations between variables by which different patterns can be identified and analyzed. It is a useful way of determining similarity of an unknown sample set to a known one. It differs from Euclidean distance in that it takes into account the correlations of the data set. The Mahalanobis distance from a group of values with mean $\mu = (\mu_1, \mu_2, \mu_3, \mu_4 \ldots, \mu_n)$ and covariance matrix Σ for a multivariate vector $x = (x_1, x_2, x_3, x_4 \ldots, x_n)$ is,

$$D_M(x) = \sqrt{(x-\mu)^T \Sigma^{-1} (x-\mu)} \quad (4)$$

Mahalanobis distance can also be defined as dissimilarity measure between two random vectors $\vec{x}$ and $\vec{y}$ of the same distribution with the covariance matrix Σ,

$$d(\vec{x}, \vec{y}) = \sqrt{(\vec{x}-\vec{y})^T \Sigma^{-1} (\vec{x}-\vec{y})} \quad (5)$$

The Mahalanobis distance approach has been chosen over other classification approaches as it considers the variance and covariance of the variables as opposed to only the average value. The distance measure is taken as a basis for the calculation of the confidence values for prognostics.

Closed-Form Modeling Approach
for Free-Drop of PCA with Component-Masses

In this section, a closed-form modeling approach has been used to analyze the dynamic behavior of printed circuit assembly with component masses. The Lagrangian Functional for a rectangular printed-circuit assembly is,

$$L = \int_0^a \int_0^b \left\{ \begin{array}{l} \frac{D}{2}\left[\left(\frac{\partial^2 W_o}{\partial x^2} \right)^2 + \left(\frac{\partial^2 W_o}{\partial y^2} \right)^2 + 2\nu \frac{\partial^2 W_o}{\partial x^2} \frac{\partial^2 W_o}{\partial y^2} \right. \\ \left. + 2(1-\nu)\left(\frac{\partial^2 W_o}{\partial x \partial y} \right)^2 \right] \\ + qW_0 - \left(\frac{1}{2} \right) \left\{ \begin{array}{l} I_0 (\dot{W}_0)^2 \\ + I_2 \left[\left(\frac{\partial \dot{W}_0}{\partial x} \right)^2 + \left(\frac{\partial \dot{W}_0}{\partial y} \right)^2 \right] \end{array} \right\} \end{array} \right\} dxdy \quad (6)$$

Where, W_0 is the Mode shape Functional, E is the elastic modulus, ν is the Poisson's Ratio, h is the thickness of the printed-circuit board, a is the length of the PCB, b is the width of the PCB, q is the distributed loads on the PCB, ρ is the density of the PCB, D is the flexural rigidity, I_0 and I_2 are the mass moments-of-inertia.

$$\begin{Bmatrix} I_0 \\ I_2 \end{Bmatrix} = \int_{\frac{-h}{2}}^{\frac{h}{2}} \begin{Bmatrix} 1 \\ z^2 \end{Bmatrix} \rho dz = \rho_0 \begin{Bmatrix} h \\ h^3/12 \end{Bmatrix} \quad D = \frac{Eh^3}{12(1-\nu^2)} \quad (7)$$

For the free vibration of the printed circuit board, the force applied on the PCB is zero, i.e. q = 0, and neglecting the rotary inertia to be zero, i.e. $I_2 = 0$. The Euler-Lagrange equation or the Governing Differential equation for free vibration of an orthotropic rectangular PCB is given by,

$$\Rightarrow \left(D_{11} \frac{\partial^4 W_0}{\partial x^4} + 2(D_{66} + 2D_{12}) \frac{\partial^4 W_0}{\partial x^2 \partial y^2} + D_{22} \frac{\partial^4 W_0}{\partial y^4} \right) + \frac{\partial}{\partial x}\left(N_{xx} \frac{\partial W_0}{\partial x} + N_{xy} \frac{\partial W_0}{\partial y} \right) + \frac{\partial}{\partial y}\left(N_{xy} \frac{\partial W_0}{\partial x} + N_{yy} \frac{\partial W_0}{\partial y} \right) = q - I_0 \ddot{W}_0 + I_2 \left(\frac{\partial^2 \ddot{W}_0}{\partial x^2} + \frac{\partial^2 \ddot{W}_0}{\partial y^2} \right) \quad (8)$$

The following functional form has been used for Rayleigh-Ritz solution from set of admissible functions for the rectangular plate-strip,

$$W_o(x, y, t) = W(x, y) e^{i\omega t} \quad (9)$$

where ω is the natural frequency at which the plate vibrates when the mode shape of the plate is given by $W(x, y)$ is assumed. The governing differential equation of printed circuit strip in the absence of transverse shear forces, normal edge moments, and tensile and compressive forces,

$$D \frac{\partial^4 W_0}{\partial x^4} = I_2 \frac{\partial^4 W_0}{\partial x^2 \partial t^2} - I_0 \frac{\partial^2 W_0}{\partial t^2} - \hat{N}_{xx} \frac{\partial^2 W_0}{\partial x^2} \quad (10)$$

The solution can be expressed as

$$W(x) = c_1 \sin \frac{\varepsilon x}{L} + c_2 \cos \frac{\varepsilon x}{L} + c_3 \sinh \frac{\varepsilon x}{L} + c_4 \cosh \frac{\varepsilon x}{L} \quad (11)$$

where

$$\frac{\varepsilon^2}{L^2} = \sqrt{\frac{\omega^2 I_o}{D}} \quad (12)$$

The free-drop of a printed circuit assembly has been solved by superimposing the FF printed circuit strip solutions along the x-direction and y-directions. The mode shape functional for the rectangular plate is expressed as a product using separation of variables,

$$W(x, y) = A_{mn} X_m(x) Y_n(y) \quad (13)$$

where $X_m(x)$ and $Y_n(y)$ are the mode-shape functionals of the printed-circuit board strips which have the boundary conditions of the plate in the x direction and the y direction respectively. The approximation function used for solution of the weak form are,

$$X_1(x) = 1 \qquad X_2(x) = \sqrt{3}\left(1 - \frac{2x}{a}\right)$$

$$X_m(x) = \left[\cosh \frac{\varepsilon_m x}{a} + \cos \frac{\varepsilon_m x}{a} - \alpha_m \left(\sinh \frac{\varepsilon_m x}{a} + \sin \frac{\varepsilon_m x}{a} \right) \right]$$

$$m = 3,4,5,7\ldots. \quad (14)$$

Where, α_m is calculated from,

$$\alpha_m = \frac{\cosh \varepsilon a - \cos \varepsilon a}{\sin \varepsilon a - \sinh \varepsilon a} \quad (15)$$

$$Y_1(y) = 1 \qquad Y_2(y) = \sqrt{3}\left(1 - \frac{2y}{b}\right)$$

$$Y_n(y) = \left[\cosh \frac{\varepsilon_n y}{b} + \cos \frac{\varepsilon_n y}{b} - \alpha_n \left(\sinh \frac{\varepsilon_n y}{b} + \sin \frac{\varepsilon_n y}{b} \right) \right]$$

$$n = 3,4,5,7\ldots. \quad (16)$$

Where, α_n is calculated from,

$$\alpha_n = \frac{\cosh \varepsilon b - \cos \varepsilon b}{\sin \varepsilon b - \sinh \varepsilon b} \tag{17}$$

Where ε is calculated from the transcendental equation, $\cosh \varepsilon \cos \varepsilon - 1 = 0$ for both Equations (15) and (17). The following boundary conditions for the FFFF rectangular printed circuit assembly have been imposed,

$$\left.\begin{aligned} M_{xx} &= -D\frac{\partial^2 W}{\partial x^2} = 0 \\ V_x &= -D\frac{\partial^3 W}{\partial x^3} = 0 \end{aligned}\right\} \text{at } x = 0, a \qquad \left.\begin{aligned} M_{yy} &= -D\frac{\partial^2 W}{\partial y^2} = 0 \\ V_y &= -D\frac{\partial^3 W}{\partial y^3} = 0 \end{aligned}\right\} \text{at } y = 0, b \tag{18}$$

The assumed solution is applied to the weak form of the GDE,

$$\delta\Pi = \int_0^a \int_0^b \left\{ D\left[\begin{aligned} &\frac{\partial^2 W_0}{\partial x^2}\frac{\partial^2 \delta W_0}{\partial x^2} \\ &+ \nu\left(\frac{\partial^2 W_0}{\partial y^2}\frac{\partial^2 \delta W_0}{\partial x^2} + \frac{\partial^2 W_0}{\partial x^2}\frac{\partial^2 \delta W_0}{\partial y^2} \right) \\ &+ 2(1-\nu)\frac{\partial^2 W_0}{\partial x \partial y}\frac{\partial^2 \delta W_0}{\partial x \partial y} \\ &+ \frac{\partial^2 W_0}{\partial y^2}\frac{\partial^2 \delta W_0}{\partial y^2} \end{aligned} \right] - \left(I_o \ddot{W}_0 \delta W_0\right) \right\} dxdy \tag{19}$$

$$\delta\Pi = \sum_{i=1}^{m}\sum_{j=1}^{n} \frac{\partial \Pi}{\partial A_{ij}} \delta A_{ij} \tag{20}$$

The Ritz method states that for {A} to be linearly independent

$$\frac{\partial \Pi}{\partial A_{ij}} = 0 \qquad \text{for } i = 1, 2.....m;\ j = 1, 2....n \tag{21}$$

Assuming

$$W_0 = \sum_{i=1}^{p}\sum_{j=1}^{q} A_{ik} X_i Y_k \qquad \delta W_0 = \sum_{p=1}^{p}\sum_{q=1}^{q} \delta A_{mn} X_m Y_n \tag{22}$$

Applying the Ritz Method, we can represent the vibration problem as an Eigenvalue problem,

i.e. $C_{mn}^{(ik)} - \lambda \delta_{mn} = 0$, where

$ik = mn$

$$C_{mn}^{(ik)} = \left[\begin{aligned} &\frac{b\varepsilon_i^4}{2a} + \frac{a^3(k\pi)^4}{2b^3} \\ &+ 2\frac{a}{b}\nu\left(\int_0^a X_i \frac{d^2 X_i}{dx^2} dx \right)\left(\int_0^b Y_k \frac{d^2 Y_k}{dy^2} dy \right) \\ &+ 2(1-\nu)\frac{a}{b}\left(\int_0^a \frac{dX_i}{dx}\frac{dX_i}{dx} dx \right)\left(\int_0^b \frac{dY_k}{dy}\frac{dY_k}{dy} dy \right) \end{aligned} \right]$$

$ik \neq mn$

$$C_{mn}^{(ik)} = \left[\begin{aligned} &\frac{a}{b}\nu\left(\int_0^a X_i \frac{d^2 X_m}{dx^2} dx \right)\left(\int_0^b Y_n \frac{d^2 Y_k}{dy^2} dy \right) \\ &+ \left(\int_0^a X_m \frac{d^2 X_i}{dx^2} dx \right)\left(\int_0^b Y_k \frac{d^2 Y_n}{dy^2} dy \right) \\ &+ 2(1-\nu)\frac{a}{b}\left(\int_0^a \frac{dX_i}{dx}\frac{dX_m}{dx} dx \right)\left(\int_0^b \frac{dY_k}{dy}\frac{dY_n}{dy} dy \right) \end{aligned} \right] \tag{23,24}$$

$$\lambda = \frac{\omega^2 I_0 a^3 b}{2D} \tag{25}$$

Point Masses at Location of Components

Mode superposition [Clough, et. al. 1975] has been used to represent the out-of-plane displacement, $W(x, y, t)$ due to forced vibration

$$W(x, y, t) = \sum_{i=1}^{n'} \overline{W}_i(x, y)\, q_i(t) \tag{26}$$

where $\overline{W}_i(x, y)$ is the i^{th} normal mode shape of the unconstrained plate, $q_i(t)$ is the i^{th} generalized co-ordinate, and *n'* is the mode number. The mode shapes are arranged in order of the modal frequency. The assumed solution is substituted into the equation for the rectangular orthotropic plate,

$$\begin{aligned} &\left(D_{11}\frac{\partial^4 W_0}{\partial x^4} + 2(D_{66} + 2D_{12})\frac{\partial^4 W_0}{\partial x^2 \partial y^2} + D_{22}\frac{\partial^4 W_0}{\partial y^4} \right) \\ &+ \frac{\partial}{\partial x}\left(N_{xx}\frac{\partial W_0}{\partial x} + N_{xy}\frac{\partial W_0}{\partial y} \right) \\ &+ \frac{\partial}{\partial y}\left(N_{xy}\frac{\partial W_0}{\partial x} + N_{yy}\frac{\partial W_0}{\partial y} \right) \\ &= q - I_0 \ddot{W}_0 + I_2\left(\frac{\partial^2 \ddot{W}_0}{\partial x^2} + \frac{\partial^2 \ddot{W}_0}{\partial y^2} \right) \end{aligned} \tag{27}$$

Pre-multiplying both sides of the resulting equation by $\overline{W}_j(x, y)$ and integrating the expression over area, A, of the plate, and using orthogonality,

$$\overline{M}_{jj}\ddot{q}_j(t) + \overline{K}_{jj} q_j(t) = \overline{P}_j(t), \qquad j = 1, \ldots n' \tag{28}$$

Where,

$$\begin{aligned} \overline{M}_{jj} &= \int_A \overline{W}_j \rho\, \overline{W}_j\, dA \\ \overline{K}_{jj} &= \int_A \overline{W}_j D_E \nabla^4 \overline{W}_j\, dA \\ \overline{P}_j(t) &= \int_A q(x, y, t)\, \overline{W}_j\, dA \end{aligned} \tag{29}$$

If, $\overline{W}_j(x, y)$ is the normal mode shape w.r.t. ρ, then $\overline{M}_{jj} = 1$, and the GDE can be simplified into [Wu, et. al. 1997a, b],

$$\begin{aligned} &\ddot{q}_j(t) + \omega_j^2 q_j(t) = \overline{P}_j(x_a, y_a, t)\overline{W}_j(x_a, y_a) \\ &j = 1, \ldots n' \end{aligned} \tag{30}$$

The governing differential equation for a rectangular plate has been modified to represent the location of devices on the printed circuit board with addition of point masses [Wu, et. al. 1997a, b], as follows

$$\overline{P}(x_a, y_a, t) = -kW(x_b, y_b, t) - m\frac{\partial^2 W(x_a, y_a, t)}{\partial t^2}$$
$$= -k\sum_{i=1}^{n'} \overline{W}_i(x_b, y_b) q_i(t) - m\sum_{i=1}^{n'} \frac{\partial^2 q_i(t)}{\partial t^2} \overline{W}_i(x_a, y_a) \quad (31)$$

where m is the point mass at (x_a, y_a) and k is the spring constant of the spring present at point (x_b, y_b) on the rectangular plate. The spring stiffness is intended to model supports. Hence the equation of motion obtained for a constrained plate is

$$\ddot{q}_j(t) + \omega_j^2 q_j(t) = -m\overline{W}_j(x_a, y_a)\sum_{i=1}^{n'} \overline{W}_i(x_a, y_a)\ddot{q}_i(t)$$
$$- k\overline{W}_j(x_a, y_a)\sum_{i=1}^{n'} \overline{W}_i(x_a, y_a) q_i(t) \quad (32)$$

$j = 1, \ldots n'$

Model Based Correlation of Damage with Degradation in Confidence Value

The closed form modeling approach described above shows us the affect of the change in effective parameters on the reliability of the confidence values. To provide a physical relevance to the above approach an explicit finite element model for the free drop of a The 0.5 mm pitch, 132 I/O, 8 mm flex-substrate CSP has been created.

A reduced integration shell elements (S4R) is used for the PCB, and the various component layers such as the substrate, die attach, silicon die, mold compound have been modeled with C3D8R elements. The interconnects are modeled using two-node beam elements (B31) in place of solder balls as shown in Figure 6 and Figure 7. Smeared properties have been derived for the CSP considering all the individual components mentioned above. The concrete floor has been modeled using rigid R3D4 elements. A weight has been attached on the top edge of the board.

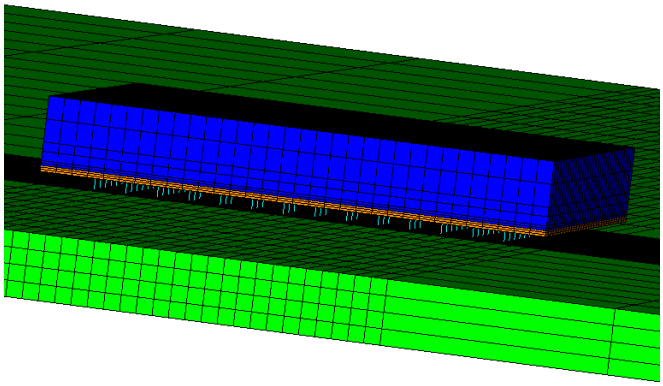

Figure 6 Package with Solder Beam Array

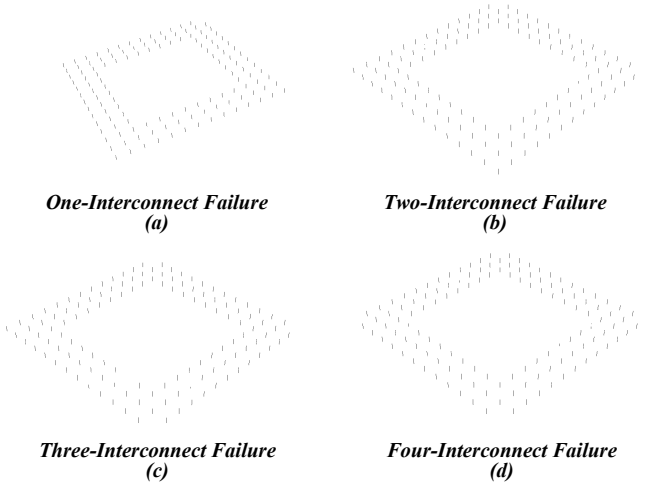

Figure 7: Model Configurations for Correlation of Damage to Confidence Value Degradation.

The above described model for the free drop was analyzed several times, with all solder beams intact and with various corner solder beams failed. The statistical pattern recognition methods described in this paper have been applied to the time history output of the strain signal obtained at the PCB surface below the centre of the package, where the sensor would have been mounted in an experimental setup. The confidence values computed as shown in Figure 8, show degradation of reliability with solder ball failure thus showing the applicability of the above stated damage monitoring methods to the reliability studies of Electronic assemblies.

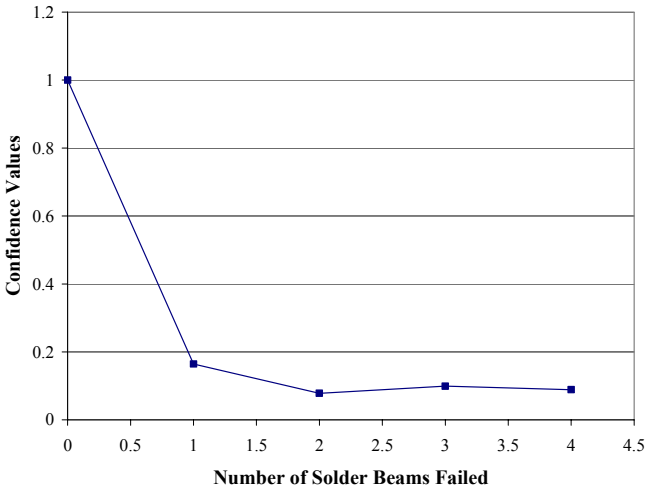

Figure 8 Confidence Value degradation in Transient PCB Strain with Solder Ball Failure

Computation of Confidence Value with Damage Progression

The damage monitoring of electronic assemblies by statistical pattern recognition has been applied to experimental results obtained by the JESD22-B11 drop and shock testing of PCB011. The boards were thermal cycled for 750 cycles and then subjected to JEDEC drop testing.

The strain signal obtained from sensors placed on the board at appropriate locations are employed to perform statistical pattern recognition. The feature vectors as shown in Figure 9 used in failure pattern classification are seen to show significant change in case of failure of a package irrespective to the placement of the sensor.

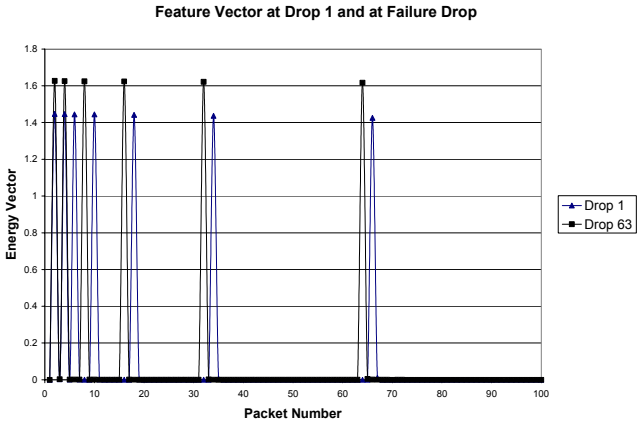

Figure 9 Feature Vector used in Failure Classification.

Statistical pattern recognition has been applied to the strain signals taken at the various drops of the board. A linear regression fit of the confidence values obtained show a progressive degradation of reliability of the assembly with the number of drops. A significant drop of reliability occurs with failure of individual packages on the assembly. The confidence value plots, as shown in Figure 10, computed by statistical pattern recognition of strain signals obtained from the strain sensors show a good correlation of the reliability degradation with the experimental values. The above correlation is performed to exhibit the applicability of statistical pattern recognition techniques to monitor damage progression in experimental setups. The degradation in confidence values demonstrates the capability of the approach in sensing damage progression and failure at the same location and other locations in the board assembly. Package-3 transient strain degradation in confidence value because of failure at package location-1. Package-1 transient strain shows degradation in confidence value due to failure at package location-1 and package-location-3.

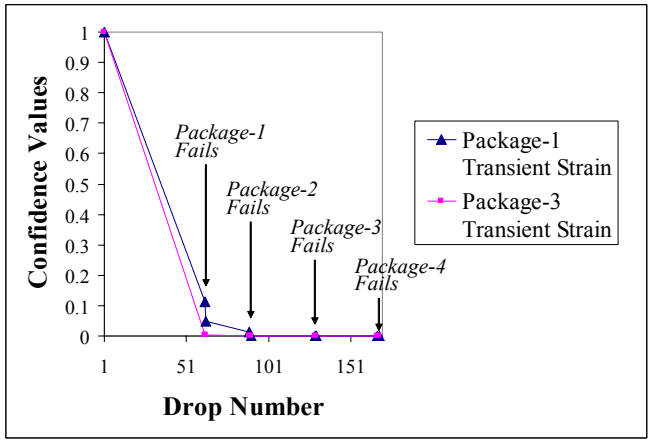

Figure 10 Confidence value degradation showing progressive damage with the Drops

Effect of Changing BCs using Closed-Form Models

Closed form models are used to study the damage progression in electronic devices at product-level. Damage progression has been monitored through correlating changes in structural parameters with the dynamic response of the assembly. Effective parameter changes implying damage in an electronic assembly include, changes in flexural rigidity, changes in effective properties, and the change in boundary conditions.

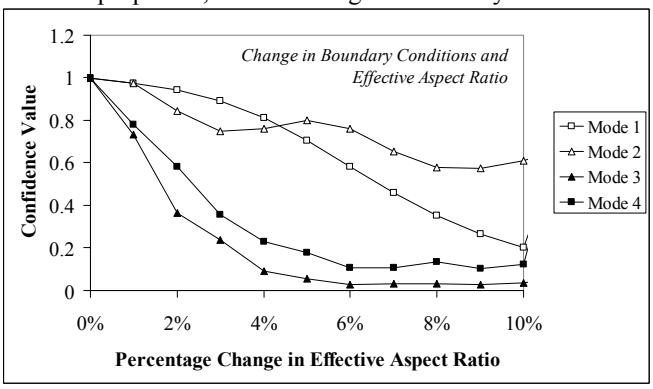

Figure 11 Damage Detection for change in Boundary conditions coupled with change in effective Aspect Ratio.

Partial release or complete failure of constraints may produce change in the aspect ratio or eventual shift of boundary conditions of the assembly. Further, failure of the interconnects or fall-off of the components may produce changes in the flexural rigidity and smeared properties of the PCA. Case study has been analyzed using closed-form models, in which the PCB is press fitted in a product casing, which might open due to shock and drop causing the boundary conditions for vibration to change from clamped to free conditions. Clamped condition can be realized in a product with a printed circuit assembly in which the printed circuit assembly is held between two snap-fit housings. In the example case-study, the boundary conditions gradually change to FFFF, from CFFF in the original assembly. The confidence value degradation for change in boundary conditions is quite significant as shown in Figure 11.

Conclusions

In this paper an approach for health monitoring in electronic products, based on closed-form energy-method based models, explicit finite elements, and statistical pattern recognition has been developed. Statistical pattern recognition techniques previously employed in several engineering and scientific disciplines such as biology, psychology, medicine, marketing, artificial intelligence, computer vision and remote sensing, have been used for monitoring damage progression in electronic assemblies. Damage proxies have been developed based on the Wavelet Packet Energy and the Mahalanobis Distance approach applications to the experimental and simulation data. The above approach addresses detection and monitoring of shock-even damage, without requiring continuous high-speed interconnect resistance monitoring during drop and shock events. Detected changes in damage have been demonstrated with changes in the energy feature vector and the change in the confidence value of the signal. The approach has been demonstrated for several test cases

including failure of one-or-more interconnects in an area-array package, failure of packages at the location of transient-strain measurement or at another location, and change in the structural properties and the transient dynamic response of the structure.

Acknowledgements

The research presented in this paper has been supported by the Grant Number ECS-0400696 from the National Science Foundation.

References

Akay, M., Wavelet Applications in Medicine, IEEE Spectrum, Vol: 34 , Issue: 5, pp. 50 – 56, 1997.

Apte, C., Data Mining: an Industrial Research Perspective, IEEE Computational Science and Engineering, Volume 4, Issue 2, pp. 6-9, 1997.

Atlas, L., G. D. Bernard, S. B. Narayanan, Applications of Time-Frequency Analysis to Manufacturing Sensor Signals, Proceedings of the IEEE, Vol. 84, No. 9, pp. 1319-1329, 1996.

Casoetto N, Djurdjanovic D, Mayor R, Lee J, Ni J, Multisensor Process Performance Assessment through the Use of Autoregressive Modeling and Feature Maps, Transactions of SME/NAMRI, also in the SME Journal of Manufacturing Systems, Volume. 31, pp.483–90. 2003.

Castanien, K.E., Liang, C, Application of Active Structural Health Monitoring Technique to Aircraft Fuselage Structures, Proc. Smart Structures and Materials (SPIE), Volume 2721, pp. 38-49, 1996.

Christodoulou, C.I., Pattichis, C.S., Unsupervised pattern recognition for the classification of EMG signals, IEEE Transactions on Biomedical Engineering, Volume 46, Issue 2, pp. 169-178, 1999

Chuang, F., Luqing, Y., Yongqian, L., Ren, Y., Benoit, I, Yuanchu, C., Yuming, Z., Predictive Maintenance in Intelligent Control Maintenance Management System for Hydroelectric Generating Unit, IEEE Transactions on Energy Conversion, Volume 19, Issue 1, pp. 179 – 186, 2004.

Clough, R. W., Penzien, J., Dynamics of Structures, McGraw-Hill, New York, 1975.

Date, M., Shoji, T., Fujiyoshi, M., Sato, K., Tu, K.N., Impact Reliability of Solder Joints, Proceedings of the Electronic Components and Technology, Vol. 1, pp.668-674, 2004.

Dellaert, F., Polzin, T., Waibel, A., Recognizing emotion in speech, Proceedings of the Fourth International Conference on Spoken Language, Volume 3, pp.1970-1973, 1996.

Djurdjanovic D, Ni J, Lee J, Time–Frequency Based Sensor Fusion in the Assessment and Monitoring of Machine Performance Degradation., Proceedings of ASME International Mechanical Engineering Congress and Exposition, Paper number IMECE2002-2032, New Orleans, Louisiana, 2002.

Engel, S.J., Gilmartin, B.J., Bongort, K., Hess, A., Prognostics, The Real Issues Involved With Predicting Life Remaining, IEEE Aerospace. Conference Proceedings, Vol. 6, pp. 457-469, 2000.

Favero, R.F., Compound Wavelets: Wavelets For Speech Recognition, Proceedings of the IEEE-SP International Symposium on Time-Frequency and Time-Scale Analysis, pp. 600-603, 1994.

Fu, Y., Wen-Sheng Li, Guo-Hua Xu, Wavelets and Singularities in Bearing Vibration Signals, International Conference on Machine Learning and Cybernetics, Vol. 4, pp. 2433-2436, 2003.

Gorman, D.J., Free Vibration of Rectangular Plates, Elsevier-North Holland Inc., 1982.

Gurgoze, M, A Note on the Vibrations of Restrained Beams and Rods with Point Masses, Journal of Sound and Vibration, Vol. 96, No. 4, pp. 461-468, 1984

Gyekenyesi, A.L., Sawicki, J.T., and Baaklini, G.Y., Vibration Based Crack Detection in a Rotating Disk: Part 1--An Analytical Study. NASA/TM-2003-212624, 2003.

Hanabe, M., Canumalla, S., Package to Board Interconnection Shear Strength (PBISS) Behavior at High Strain Rates Approaching Mechanical Drop, Proceedings of the Electronic Components and Technology, Volume 2, pp.1263-1270, 2004.

Heck, L. P. and McClellan, J. H., Mechanical System Monitoring Using Hidden Markov Models, Proceedings of International Conference on Acoustics, Speech and Signal Processing, Vol. 3, pp. 1697-1700, 1991.

Hedley, M., Hoschke, N., Johnson, M., Lewis, C., Murdoch, A., Price, D., Prokopenko, M., Scott, A., Wang, P., Farmer, A., Sensor Network for Structural Health Monitoring, Processing Conference Intelligent Sensors, Sensor Networks and Information, pp.361 – 366, 2004.

Hickman, G A, Gerardi, J J, Feng, Y, Application of smart structures to aircraft health monitoring ,Journal of Intelligent Material Systems and Structures, Vol. 2, pp. 411-430, 1991.

Holt, M., Tooley, M.A., Forest, F.C., Prys-Roberts, C., Tarassenko, L., Use of parametric modelling and statistical pattern recognition in detection of awareness during general anaesthesia, IEE Proceedings-Science, Measurement and Technology, Volume 145, Issue 6, pp. 307 – 316, 1998.

Jain, A.K., Duin, R. P. W., Mao, J., Statistical Pattern Recognition: A Review, IEEE Transactions on Pattern Analysis and Machine Intelligence, Vol.22, No.1, pp.4-37, 2000.

Kohonen, T., Barna, G., Chrisley, R., Statistical Pattern Recognition with Neural Networks: Benchmarking Studies, IEEE International Conference on Neural Networks, San Diego, CA, Vol. 1, pp.61 – 68, 1988.

Kumar, P, Georgiou, E. F., Wavelets in Geophysics, Wavelets and its Applications, Academia Press, 1994.

Lall, P., Panchagade, D., Choudhary, P., Suhling, J., Gupte, S., Failure Envelope Approach to Modeling Shock and Vibration Survivability of Electronic and MEMS Packaging, Proceedings of the Electronic Components and Technology, pp. 480 – 490, 2005.

Lau, K.-M., and H.-Y. Weng, Climate Signal Detection Using Wavelet Transform: How to Make a Time Series Sing,

Bulletin of the American Meteorological Society, No. 76, pp. 2391–2402, 1995.

Lebold, M.S., Maynard, K., Reichard, K., Trethewey, M., Bieryla, D., Lissenden, C., Dobbins, D., Using Torsional Vibration Analysis as a Synergistic Method for Crack Detection in Rotating Equipment, Proceedings of the Aerospace Conference, Volume 6, Pages: 3517-3527, 2004.

Lee, J., Machine Performance Monitoring and Proactive Maintenance in Computer-Integrated Manufacturing: Review and Perspective, International Journal of Computer Integrated Manufacturing, Vol. 8, No. 5, pp. 370-380, 1995.

Lei,.Y., Kiremidjian, A.S, Nair, K. K , Lynch, J. P., Law, K. H., An Enhanced Statistical Damage Detection Algorithm Using Time Series Analysis, Proceedings of the 4th International Workshop on Structural Health Monitoring, Stanford, Sept 15-17, pp. 1-7, 2003.

Leissa A.W., Vibration of Plates, NASA SP 160, 1969.

Logan, K. P., Prognostic Software Agents for Machinery Health Monitoring, Proceedings of the IEEE Aerospace Conference, Volume: 7, pp. 3213- 3225, March 8-15, 2003

Low, K.-C., Coggins, J.M., Biomedical Image Segmentation Using Multiscale Orientation Fields, Proceedings of the First Conference on Visualization in Biomedical Computing, pp.378 – 384, May 22-25, 1990.

Martin, M.B., Bell, A.E., New Image Compression Techniques Using Multiwavelets and Multiwavelet Packets, IEEE Transactions on Image Processing, Vol. 10, Issue: 4, pp. 500-510, 2001.

National Research Council Canada, Railway Bearing Diagnostics: Laboratory Data Analysis, 1999.

Newman, K., Brittle Fracture – Alternative Solder Joint Integraity Test Methods, Proceedings of the IEEE Electronic Components and Technology Conference, pp. 1194-1201, 2005.

Santoso, S., Powers, E.J., Grady, W.M., Hofmann, P., Power quality assessment via Wavelet transform analysis, IEEE Transactions on Power Delivery, Volume. 11 , Issue. 2, pp.. 924 – 930, 1996.

Shao,Y., Nezu, K., Prognosis of Remaining Bearing Life Using Neural Networks, Proceedings of the Institution of Mechanical Engineers, Volume 214, Part I, 2000

Sick, B., Online Tool Wear Monitoring In Turning Using Time-Delay Neural Networks, Proceedings of International Conference On Acoustics, Speech and Signal Processing, Volume. 1, pp. 445-448, 1998.

Wang, L., Mostafa G. Mehrabi, Elijah Kannatey-Asibu, Jr., Hidden Markov Model-based Tool Wear Monitoring in Turning, Journal of Manufacturing Science and Engineering, Volume 124, Issue 3, pp. 651-658, August 2002.

Wegerich, S.W., Similarity Based Modeling of Time Synchronous Averaged Vibration Signals for Machinery Health Monitoring, Proceedings of the IEEE Aerospace Conference, Big Sky, MT, pp. 3654-3662, March 6-13, 2003

Wu, J. S., Chou H-M., Chen D-W., Free vibration analysis of a rectangular plate carrying multiple various concentrated elements, Proceedings of the Institution of Mechanical Engineers, Part K: J. Multi-body Dynamics, Vol. 217, No. 2, pp. 171-183(13), 2003.

Wu, J. S., Luo, S. S., Vibration Analysis of a Rectangular Plate Carrying any Number of Point Masses and Translational Springs by Using the Modified and Quasi-Analytical and Numerical Combined Methods, International Journal for Numerical Methods in Engineering, Volume 40, pp. 2171-2193, 1997[a].

Wu, J. S., Luo, S. S., Use of the analytical and Numerical Combined Method in the Free Vibration Analysis of a Rectangular Plate with any Number of Points Masses and Translational Springs, Journal of Sound and Vibration, Volume 200, No. 2, pp. 179-194, 1997[b].

Yan, J., Lee J., Degradation Assessment And Fault Modes Classification Using Logistic Regression, Journal of Manufacturing Science and Engineering, Volume 127, Issue 4, pp. 912-914, November 2005.

Yan, J.., Koc M., Lee J., A Prognostic Algorithm For Machine Performance Assessment and its Application, Production Planning and Control, Vol. 15, No. 8, pp. 796–801, 2004,

Yen, G.Y., Kuo-Chung Lin, Wavelet Packet Feature Extraction For Vibration Monitoring, Proceedings of the 1999 IEEE International Conference on Control Applications, Vol.2, pp. 1573 - 1578, 1999.

Young, D, Vibration of the Rectangular plates by the Ritz Method, Journal of Applied Mechanics, Vol. 17, pp. 448-453, 1950.

Yuan, S., Ge M, Qiu H, Lee J, Xu Y, Intelligent Diagnosis In Electromechanical Operations Systems, Proceedings of 2004 IEEE International Conference on Robotics and Automation, pp. 2267–72, 2004.

Zheng, K. and Whitehouse, D. J., The Application of the Wigner Distribution to Machine Tool Monitoring, Proceedings of the Institution of Mechanical Engineers, Vol. 206, pp 249-264, 1992.